The Short- and Long-Term Mechanical Properties of Filled and Unfilled Thermotropic Liquid Crystalline Polymer Injection Moldings

C. J. G. PLUMMER,[1]* Y. WU,[1] P. DAVIES,[2] B. ZÜLLE,[3] A. DEMARMELS,[3] and H.-H. KAUSCH[1]

[1]Laboratoire de Polymères, Ecole Polytechnique Fédérale de Lausanne, CH-1015 Lausanne, Switzerland; [2]Laboratoire de Matériaux, Institut Français de Recherche pour l'Exploitation de la Mer (IFREMER), Centre de Brest, BP70, 29280 Plouzané, France; [3]Asea Brown Boveri, Corporate Research CRBV, CH-5405 Baden-Dättwil, Switzerland

SYNOPSIS

The basic mechanical properties of a series of injection moldings of the thermotropic liquid crystalline polymer Vectra have been investigated to determine the effect of fillers on the short- and long-term mechanical properties of these materials. Mineral-filler addition results in a slight decrease in strength and an increase in stiffness in the flow direction, but has relatively little effect on the anisotropy. Glass fiber addition, on the other hand, may substantially lower the anisotropy depending on the degree of fiber orientation transverse to the flow direction. The glass fiber-filled grade investigated also showed improved creep properties at high temperature compared with both the unfilled and mineral-filled grades.

INTRODUCTION

Structural *thermotropic liquid crystalline polymers* (TLCPs) are a relatively new class of materials, whose commercial development had its beginnings in the mid-1970s,[1-3] since which time most leading polymer producers have at some stage invested in their development.[4-6] Commercial TLCPs are characterized by highly rigid linear chains, typically incorporating benzene and naphthalene units, as is the case of the Vectra™ "A" series of filled and unfilled random copolymers studied here, whose composition is 73%/27% hydroxybenzoic acid–hydroxynaphthoic acid (HBA–HNA), with a main melting point of approximately 280°C.

Such materials differ radically from conventional polymers in that their molecules undergo spontaneous local alignment in the melt state to form a liquid crystalline phase. This, coupled with the high chain rigidity, leads to certain attractive features from the point of view of melt processing, including very low melt viscosities and a virtual absence of shrinkage on solidification. It is also well known that TLCPs develop significant macroscopic molecular alignment during flow and, in particular, extensional flow, which is substantially retained on solidification. Thus, TLCP injection moldings and extrudates often display exceptional mechanical properties in the flow direction, as well as extremely high levels of anisotropy and structural inhomogeneity, which are, in turn, critically dependent on the processing conditions.[7-24] To alleviate some of the problems associated with excessive anisotropy in unfilled TLCPs, the manufacturers generally recommend either mineral or short glass fiber-filled grades for injection molding. However, although it is generally recognized that the effect of fillers on the mechanical properties of these materials is less marked than in the case of conventional thermoplastics, it is not entirely clear as to the overall trends, particularly where the tensile strength is concerned.

This is for the most part due to the fact that there is no firm basis for comparing basic mechanical data from injection-molded samples with differing processing conditions and geometries and, consequently, differing molecular orientation distributions. In unfilled samples, in particular, fracture tends to initiate within a relatively highly oriented

* To whom correspondence should be addressed.

Journal of Applied Polymer Science, Vol. 48, 731–740 (1993)
 CCC 0021-8995/93/040731-10

skin region of the order of 250 μm in thickness (depending on the molding conditions). Although the skin may have a greater tensile strength than the sample interior, it is also stiffer and has a relatively low failure strain. Thus, at the point of failure, the skin is much more highly loaded than the rest of the sample, and, consequently, data for the overall stress to fail (normalized with respect to the whole sample cross section) become difficult to interpret in fundamental terms. For similar reasons, filler addition to TLCPs may result in either a decrease or an increase in tensile strength, depending on the sample geometry and on the molding conditions.[22-24] Hence, it is difficult to draw conclusions regarding the precise role of the filler directly from the results of tests on bulk samples.

In fact, measurements on individual layers cut from the TLCP moldings used in the present investigation suggest that filler addition results both in a decrease in tensile strength and an increase in modulus for a given molecular orientation.[22-24] Similar trends in the bulk room temperature tensile properties of these moldings (see below) suggest that their behavior reflects the intrinsic behavior of the material, rather than extrinsic effects relating to variations in properties within their cross sections. They were, hence, considered suitable for further bulk mechanical testing, the results of which are described in what follows. More detailed consideration of variations in their local property, structure, and orientation has been given elsewhere.[22-24]

EXPERIMENTAL

The following grades of Vectra were investigated: Vectra A950 (unfilled resin); Vectra A515 (15 wt % wollastonite-filled); Vectra A540 (40 wt % wollastonite-filled); and Vectra A130 (30 wt % short glass fiber-filled). The bulk of the tests were carried out on 3 $\times$ 6 mm^2 cross section dumbbell-shaped tensile test bars, molded with a mold temperature of 90°C and a mean barrel temperature of 280°C and at a fill-rate of 1 cm^3 s^{-1}. A limited number of 4 $\times$ 10 mm^2 cross section dumbbell-shaped tensile test bars were injection-molded at a volume fill rate of approximately 10 cm^{3}s^{-1} and with mean melt and mold temperatures of 280 and 80°C, respectively. Also investigated were various plaque samples of Vectra, injection-molded by Atochem and by Hoechst AG.

Tensile and creep testing was carried out using a Zwick tensile test apparatus, equipped with an environmental chamber. For the creep tests, 200 s compliance–stress curves were measured at low strains to determine the range of linearity, and in consequence, the applied load was fixed at 50 N (2.8 MPa) for the small strain measurements. Owing to the scatter in modulus within a given batch of samples, a single sample was used for each set of measurements over the chosen temperature range, being subsequently relaxed *in situ* for five times the duration of the previous test (to avoid disturbing the sample and the extensometer) and then conditioned for 5 h at the new test temperature. Room temperature creep measurements at higher loads and creep rupture tests made use of the Schenck tensile test apparatus, and additional creep rupture data for longer loading times were obtained from dead weight tests.

In fracture mechanics tests, the European Structural Integrity Society Protocol for fracture toughness testing was followed. Single-edge notch-bend specimens were cut from 100 $\times$ 100 $\times$ 5 mm Vectra A950 and Vectra A130 plaques (Atochem) at various orientations to the main flow direction, and precracks were introduced into the tip of the notch using a single pass with a new razor blade. Some impact tests were also carried out on both the Frank and the CEAST pendulum apparatus.

RESULTS

Tensile Tests

Dumbbell Samples

The results of simple tensile testing are given in Figure 1 for the 3 $\times$ 6 and 4 $\times$ 10 mm^2 tensile test bars. For all of these samples it was found that in the flow direction the tensile strength decreased and the Young's modulus increased with filler content for a given series of samples (i.e., for fixed molding conditions). More generally, we have found that the loss in strength appears greatest, where the molding conditions are such that the strength of the unfilled moldings is relatively high (approaching 200 MPa).[22] Whereas the strength of the unfilled moldings is lower as in the case of the 4 $\times$ 10 mm^2 moldings, the filler has less effect on the strength, although modulus reinforcement is still evident.

Addition of 30% glass fiber to the 3 $\times$ 6 mm^2 samples resulted in a decrease in the room temperature tensile strength in the flow direction from approximately 200 to 170 MPa, consistent with the results of Voss and Friedrich for 3.2 mm-thick plaques,[25] but not with the suppliers' data for 4 mm-

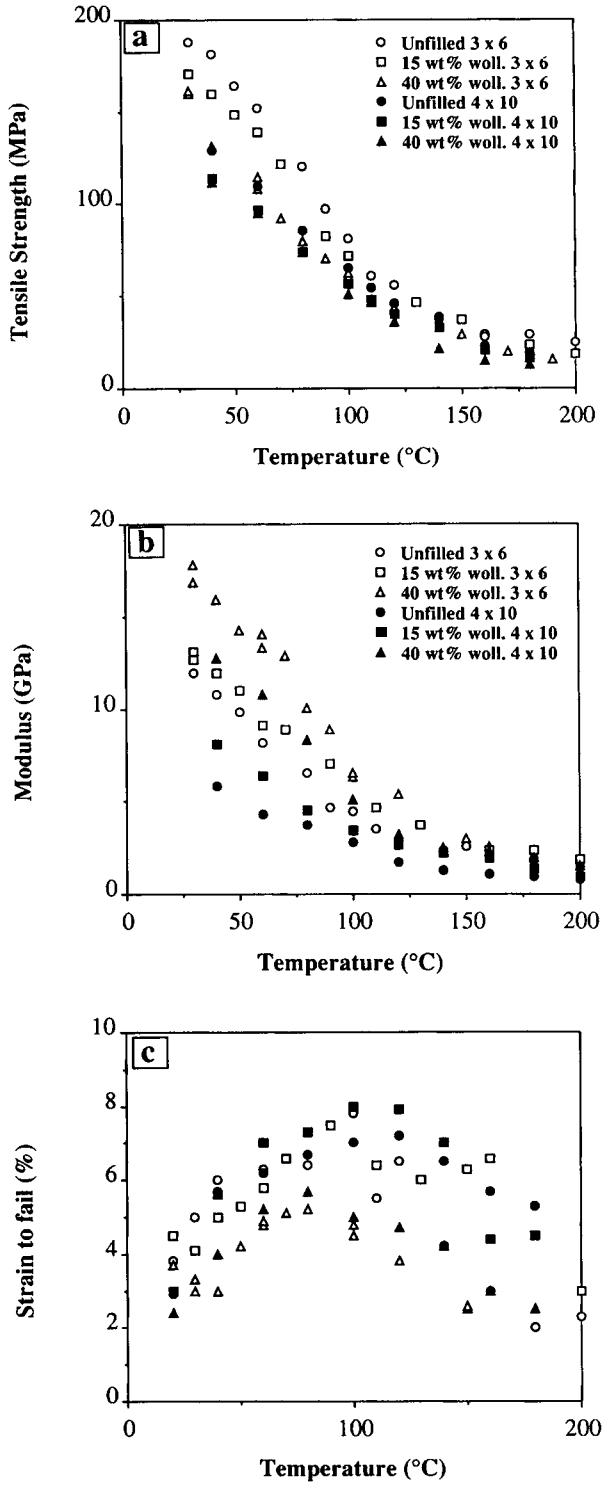

Figure 1 Wollastonite filler content and mechanical properties in test bars of Vectra for two different cross sections (crosshead speed 10 mm/min): (a) tensile strength as a function of T; (b) Young's modulus as a function of T; (c) stress to fail as a function of T [symbols as (a) throughout].

thick samples, which indicate an increase from 156 to 188 MPa, or with our own results for the 2 mm-thick plaques to be described in the next section, for which there was an increase from 145 to 150 MPa.

The results in Figure 1 also illustrate the steep drop in modulus and tensile strength with T between room temperature and approximately 100°C and a corresponding peak in the strain to fail at approximately 100°C. This temperature appears to be associated with a second-order transition,[26] visible, e.g., in DSC scans.

Plaque Samples

The effect of orientation of the tensile test direction on mechanical properties in filled and unfilled injection moldings is illustrated in Figures 2 and 3 for 2 and 4 mm-thick edge-gated 80 × 80 mm^2 plaques. The details of the molding of similar plaques are discussed in Ref. 27; here, we assume uniform properties across the sample width, consistent with microscopical observation of little change in microstructure within the plane of the plaques. The data given are the static tensile strength and the Young's

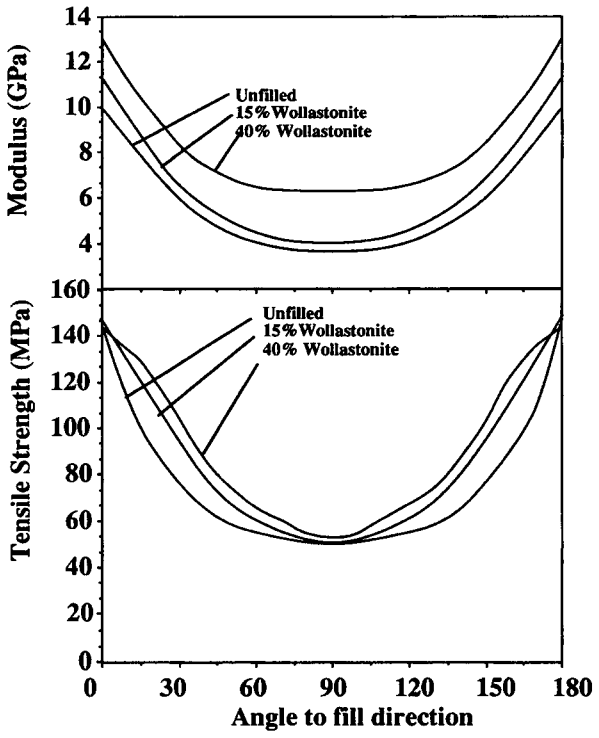

Figure 2 Anisotropy of tensile properties in unfilled and mineral-filled 2 mm-thick plaques (crosshead speed 2 mm/min).

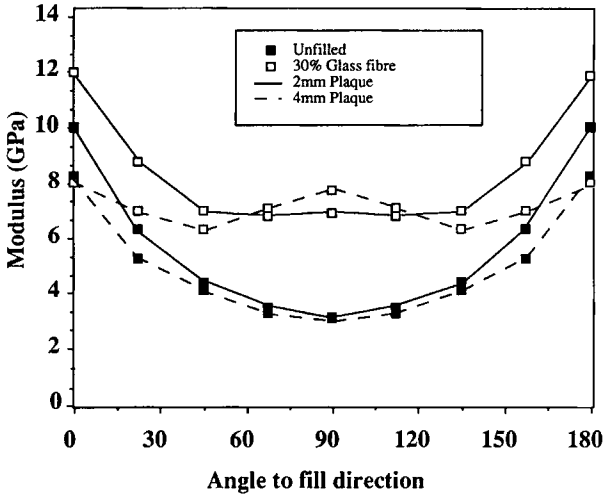

Figure 3 Anisotropy of tensile properties in 2 and 4 mm-thick unfilled and glass fiber-filled plaques (crosshead speed 2 mm/min).

modulus measured at 2 mm/min for 5 mm-wide bars cut at different angles to the flow direction.

The addition of the particulate mineral filler results in only a modest decrease in the stiffness anisotropy of the plaques, as shown, e.g., in Figure 2, and in this case, it makes little difference to the strength anisotropy. Glass fiber addition, however, has a more marked effect, to the extent that for 4 mm-thick 30 wt % short glass fiber-filled plaques the tensile moduli perpendicular and parallel to the flow direction are very similar, with a minimum at intermediate angles. It is significant that in these particular samples a high degree of transverse orientation of the glass fibers is observed (this was not in the center of the core, where the orientation is in the flow direction, but in layers of approximately 0.7 mm in thickness and approximately 0.2 mm in from the sample surface). In the 2 mm plaques, on the other hand, for which data are also given in Figure 3, transverse orientation is restricted to a narrow central region of approximately 0.3 mm in thickness. Further, tests on thin layers machined from such plaques, not containing transverse fiber orientation, have shown similar levels of anisotropy to unfilled samples.[28]

It has been argued that where molecular alignment already results in effective fiber reinforcement addition of fibers aligned with the molecules is unlikely to have a strong influence, since the molecular and fiber modulus are of the same order of magnitude.[29] However, for transverse alignment, there is likely to be a substantial improvement in the transverse modulus, which seems a likely explanation for the large decrease in anisotropy for the 30 wt % short glass fiber-filled plaques. (The sample is effectively behaving as a cross-ply laminate and may thus retain a high degree of anisotropy at a local level.)

Acoustic Emission

The observation that addition of particle fillers lowers the strength for a given orientation[22-24] seems reasonable if one assumes the particle matrix interface itself to be a source of weakness. Certainly, from SEM of fracture surfaces, the bonding appears poor, with little matrix adhesion to the filler particles. The fact that particle fillers also break up long-range structure in the matrix seems to preclude any beneficial effect from increased delocalization of the crack front, or crack blunting, as might arise, e.g., from delamination of the coarse-layered structure in the unfilled case. Indeed, acoustic emission techniques have been used to demonstrate directly in-

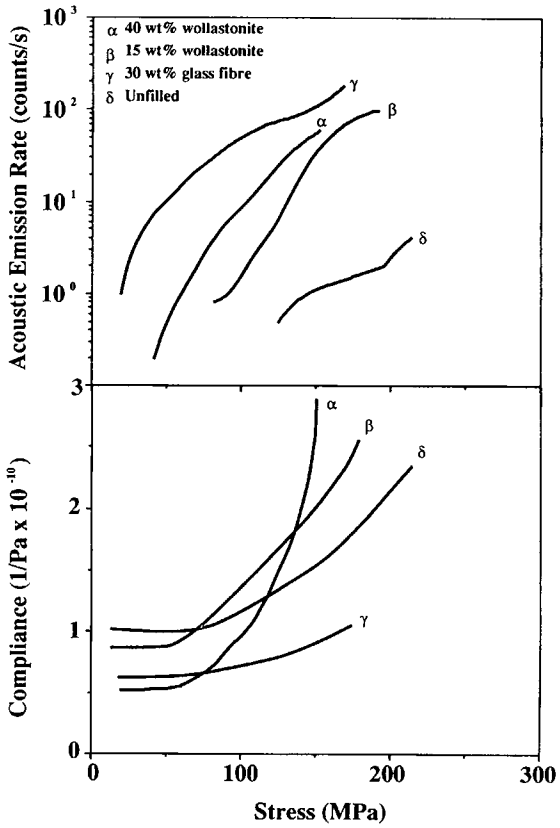

Figure 4 Acoustic emission and compliance for filled and unfilled Vectra (crosshead speed 2 mm/min).

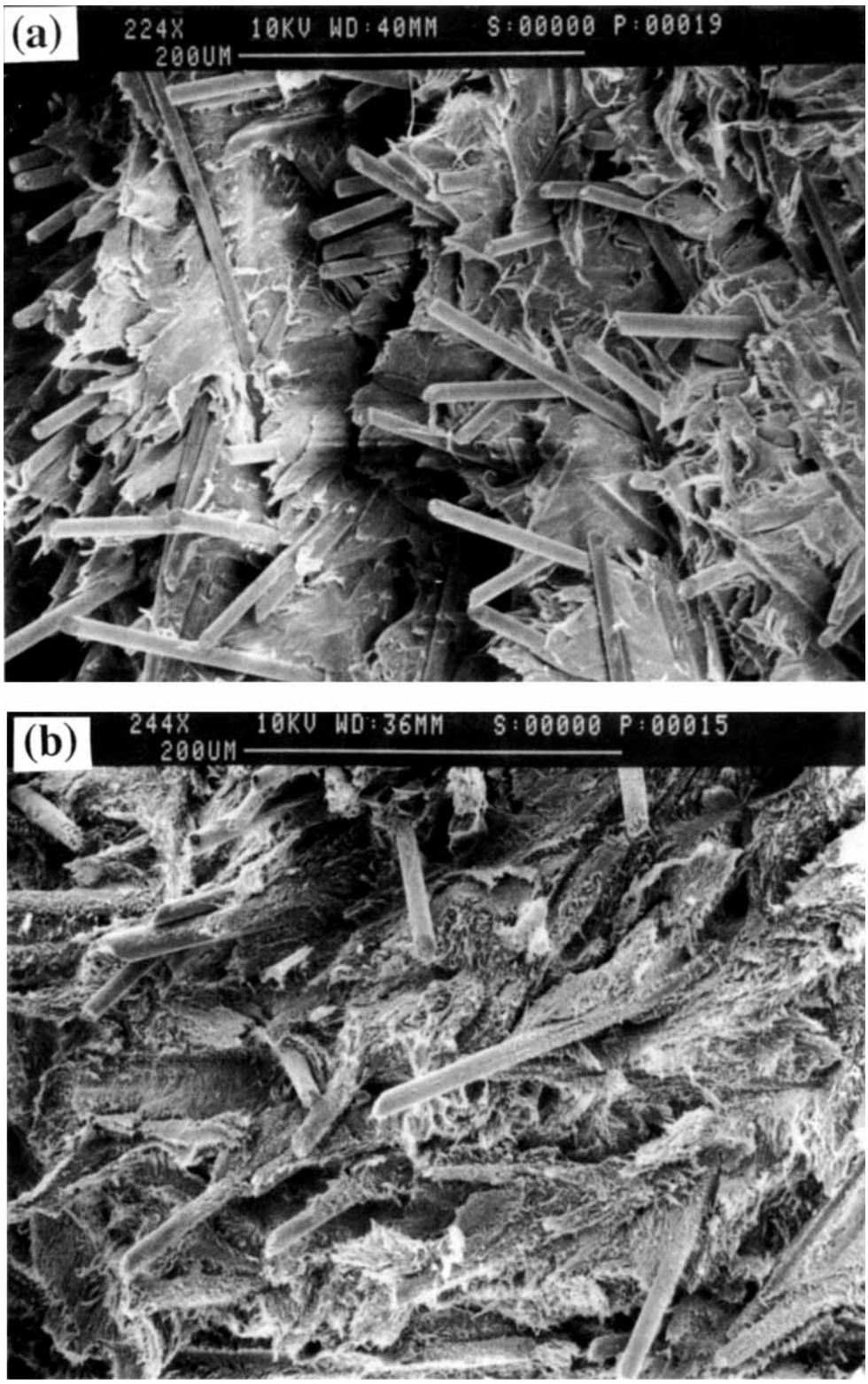

Figure 5 Fracture surfaces in glass fiber-filled Vectra: (a) skin region; (b) core region (showing slightly more matrix adhesion).

creased damage localization in notched samples on glass fiber addition to TLCPs.[30]

Our own acoustic emission measurements have been limited to attempts to monitor debonding, as shown in Figure 4 for different filler contents and for the short glass fiber-filled material (the threshold in this case was 50 dB). In the particle-filled grades, a sharp increase in acoustic emission may be identified with a considerable loss of linearity in the stress–strain curves at relatively low strains, as evidenced by the compliance–stress data given in Figure 4. For the unfilled material, substantial emission is measurable only close to the point of rupture, reflecting the greater linearity of the stress–strain curve. Indeed, at high strains, the modulus of the mineral-filled grades tends to fall below that of the unfilled material. That the damage in the mineral-filled materials is irreversible has been checked by cycling to different stresses; generally, the threshold of acoustic emission shifts to the previous highest stress level.

The behavior of the short glass fiber-filled material is somewhat different to that of the mineral-filled materials. Although the emission increases at low strains, the stress–strain curve remains approximately linear until close to failure, as in the unfilled case. Thus, while damage may be taking place, e.g., at fiber ends, or where the fibers are locally at high angles to the tensile direction, it does not greatly affect the reinforcing effect of the fibers even up to large strains, consistent with Ref. 29. Fracture surfaces (Fig. 5) nevertheless appear to indicate a high degree of fiber pullout, particularly in the outer regions.

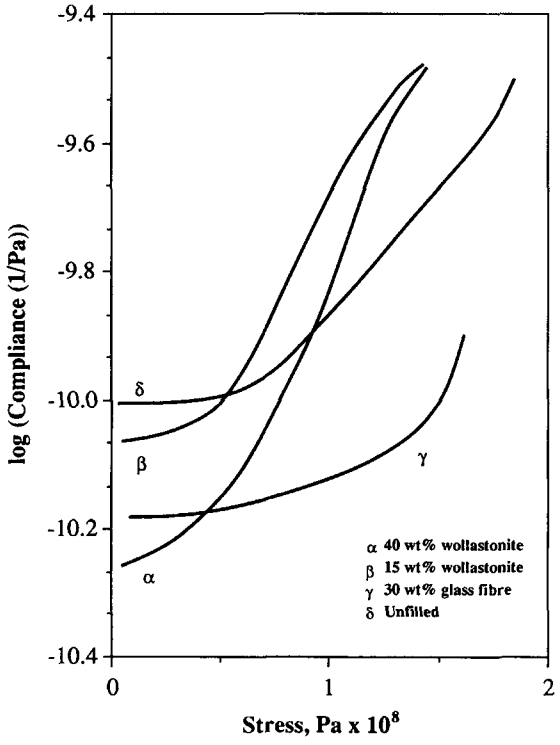

Figure 6 200 s compliance curves for 3 × 6 mm² samples.

Creep Testing

The 200 s compliance curves are shown in Figure 6, showing similar features to the tensile test curves of Figure 4 and again suggesting substantial debonding in the mineral-filled grades at stresses well below the ultimate tensile strength. Horizontal shifts have been used to superimpose the data as shown in Figure 7, along with the empirical shift factors. (Temperature scaling of the compliance would seem unjustified for rigid polymers, and the density changes are negligible.) Further, from DMA data for different frequencies in the same temperature range, it appears that only the α relaxation process at approximately 100°C, corresponding to the glass to nematic transition, is likely to influence these long term tests (Fig. 8).

The lower-temperature β peak that is clearly evident at 100 rad^{-1} moves to temperatures below room temperature for time scales associated with the creep tests. Finally, from DSC measurements, it is not believed that significant crystallization takes place in this temperature range for HBA–HNA, this being one factor that tends to mitigate against thermorheologically simple behavior in semicrystalline materials in the neighborhood of T_g.

Regardless of whether the above superposition is in any sense "valid," it provides a useful way of representing the data. If one takes the glass to crystalline/nematic transition temperature at approximately 100°C to be analogous to T_g in a conventional polymer, the overall behavior is qualitatively similar to that of semicrystalline thermoplastics.

Also given in Figure 7 are data for 40 wt % wollastonite-filled and 30 wt % glass fiber-filled moldings, shifted using the same shift factors as for the unfilled moldings. The general form of the data is similar in all three cases, but whereas there is a substantial loss of reinforcement in the mineral-filled material with increasing time or temperature, the glass fiber-filled material shows considerably improved creep properties. Indeed, the proportional modulus increase on addition of glass fibers appears to increase with time and temperature.

Creep tests have also been carried out for different

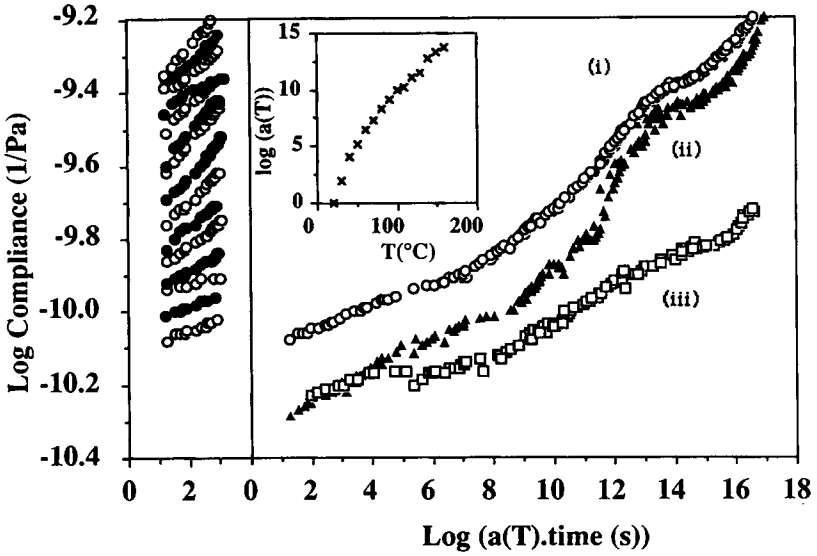

Figure 7 Compliance-time data between 23 and 160°C for an unfilled 3 × 6 mm² molding (left-hand side) and corresponding master curve [curve (i), right-hand side] obtained using the empirical shift factors shown in the inset. Curves (ii) and (iii) are master curves for 40 wt % wollastonite-filled and 30 wt % glass fiber-filled moldings, respectively, obtained using the same shift factors.

stresses for wollastonite-filled and unfilled samples. Examples are given of creep curves at different stresses in Figure 9 at room temperature. The corresponding room temperature creep rupture curves are shown in Figure 10. The similarity in slope suggests that the behavior is essentially matrix-dominated. Data have been given in Ref. 29 for similar TLCPs, including glass fiber-filled grades, showing much the same behavior.

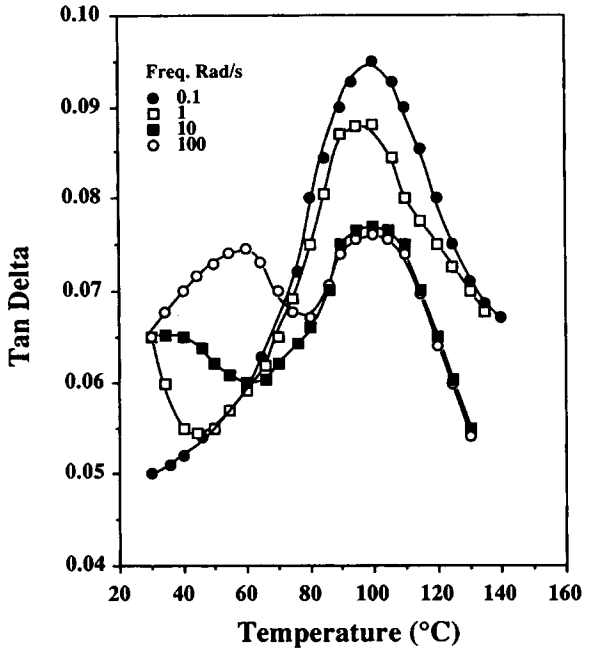

Figure 8 Tan delta as a function of frequency for unfilled 6 × 3 mm² samples in three-point bend tests (measured using the Rheometrics RSA II dynamic mechanical analyzer).

There is some evidence that the creep rupture data and static data for the tensile strength and failure strain of the 3 × 6 mm² samples may be combined to give a common failure envelope or "Smith" plot[31] as shown in Figure 11(a) (although here the stresses have not been normalized with respect to temperature). Figure 11(b) shows an attempt to superpose failure strain data at different strain rates and temperatures using the empirical shift factors obtained from the creep measurements. In spite of the scatter, there appears to be some evidence for time–temperature equivalence, the strain to fail decreasing with decreasing strain rate for $T > 100$°C (poor superposition at low temperatures might be due to the influence of the β relaxation). Correlations of this type were originally proposed for failure of rubbers, but have since been extended to other types of polymer and are generally suggestive of a fracture mechanism in which viscoelasticity has a dominant role.[32]

Fracture Toughness and Impact Testing

Our initial efforts to characterize the toughness of these materials involved impact tests. However, it

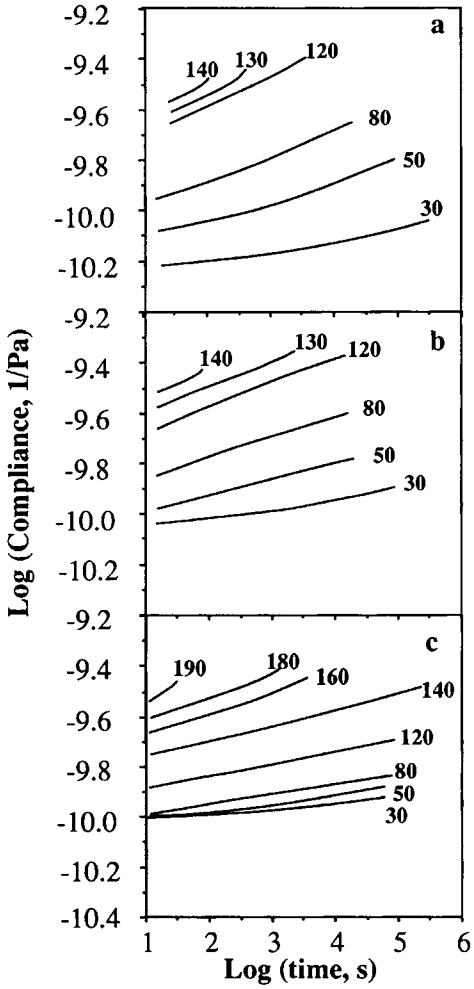

Figure 9 Creep curves at room temperature for various stresses (in Newtons): (a) 40 wt % wollastonite; (b) 15 wt % wollastonite; (c) unfilled.

proved difficult to draw more quantitative conclusions from impact data owing to sample geometry effects and notch sensitivity, factors that are compounded in the case of inhomogeneous samples such as TLCP moldings. For example, a notched impact test on a molded sample in which the notch has subsequently been cut into the surface is likely to be highly misleading, in view of the role of the skin. Indeed, notched samples of unfilled samples often simply bend on impact. This contrasts with the behavior of other thermoplastics such as PES and PEEK, for which unnotched samples tend to be most ductile under impact conditions.

In general, impact tests perpendicular to the flow direction at room T show that the unfilled moldings display very much superior toughness to the filled moldings, consistent, e.g., with the suppliers' values for the IZOD toughness (ASTM D 256) of 520 and 70 J m^{-1} for unfilled samples (Vectra A950) and 40 wt % wollastonite-filled samples (A540), respectively. In unnotched samples of the unfilled moldings, the maximum in the force displacement curve coincides with skin failure, beyond which point impact energy is absorbed by the propagation of L-shaped cracks along the fibrillar interfaces and ductile deformation of the inner part of the sample. Both mineral- and glass fiber-filled moldings, on the other hand, are found to be macroscopically brittle, i.e., the force-displacement curve drops discontinuously to zero beyond its maximum. Some multiple L-shaped cracking occurs in the surface layers, but the remainder of the sample fails by propagation of a single crack roughly perpendicular to the sample length.

Measurements of fracture toughness are also difficult since, in general, cracks do not propagate perpendicular to the flow direction. Thus, in mode I tests, crack propagation perpendicular to the load is only observed for samples loaded perpendicular to the flow direction.[25,29] We have obtained room temperature K_q values for unfilled and 30 wt % glass fiber-filled samples of 3 and 6.5 NM $m^{-3/2}$. These were measured for cracks propagating in the flow direction in single-edge notched specimens cut from 5 mm-thick injection-molded plaques (the samples in this case did not satisfy the requirements for valid K_c testing as laid down by the European Structural Integrity Society Protocol for fracture toughness testing; the ratio of P_m and $P_{5\%}$ was greater than 1.1, approaching 1.5 in some cases). These values compare with values of 3.8 and 4.1 MN $m^{-3/2}$ obtained by Chivers and Moore at −50°C,[29] suggesting a general improvement in crack resistance transverse to the flow direction on glass fiber addition.

However, such simple application of linear fracture mechanics tends not to take into account the influence of sample inhomogeneity, both on the local

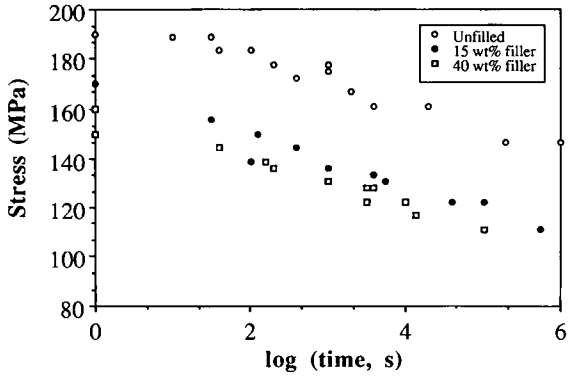

Figure 10 Room temperature creep rupture for 3 × 6 mm samples as a function of filler content.

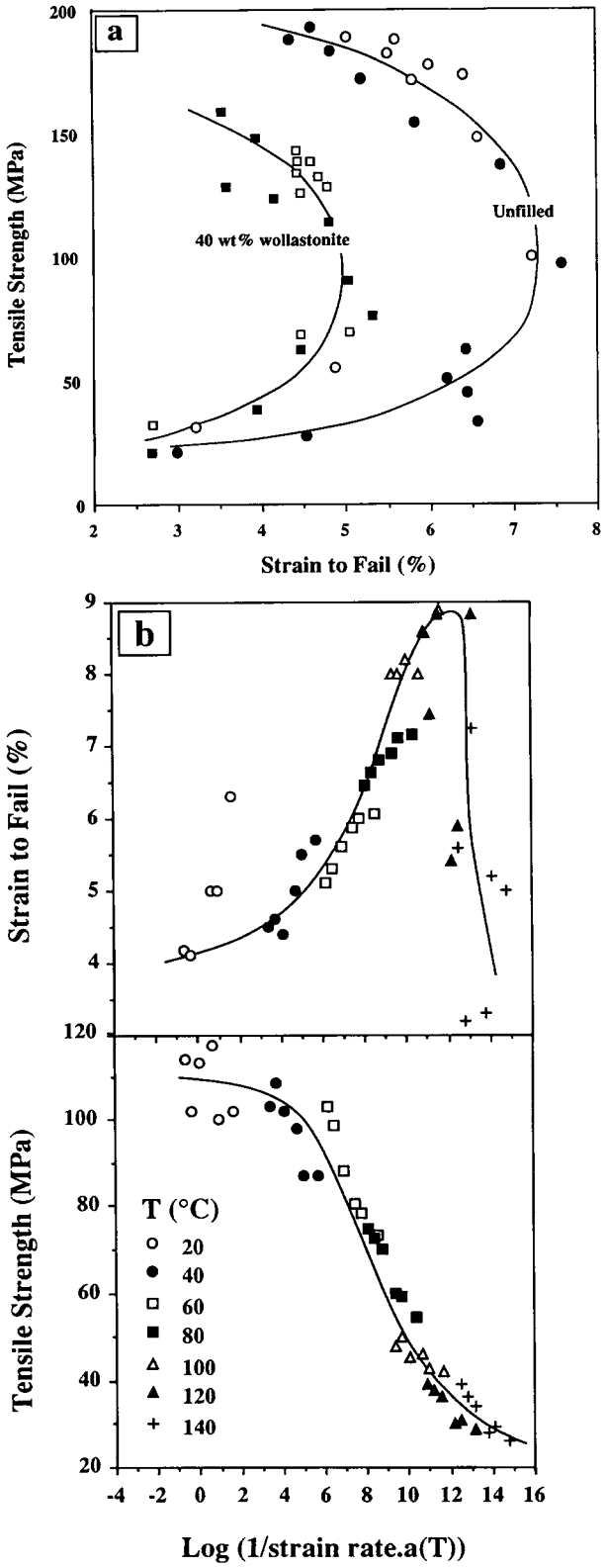

Figure 11 (a) Smith plot for 3×6 mm^2 samples: (filled symbols) static data; (open symbols) creep rupture data; (b) strain to fail and tensile strength against strain rate for unfilled 4×10 mm samples reduced to 20°C, using shift factors from Figure 7.

stresses and on the extent to which data can be considered to be true materials parameters, even where the tests conform to accepted standards. A possible approach based on measurements of modulus profiles, coupled with FEA methods, to the problem of the influence of structure in TLCP moldings has been suggested by Brew et al.[33]

CONCLUSION

For the TLCP moldings investigated during the course of this work, filler addition leads to an increase in modulus in the flow direction, at the expense of a modest decrease in tensile strength. Filled moldings are nevertheless more brittle than are unfilled moldings in impact tests, whereas the toughness of the unfilled resin as measured in IZOD tests perpendicular to the orientation direction is considerably higher than in most conventional thermoplastics. Whether this manifests itself in other types of test, such as the falling weight test, is, however, highly open to question and is an area in which we are currently working.

Particle reinforcement also tends to be ineffective at large strains, owing to poor matrix particle adhesion. This is not true of glass fiber, where reinforcement is maintained up to strains close to the failure strain and is even improved at high temperature, or long times, so that glass fiber fillers appear advantageous where creep properties are important. However, the tensile strength and modulus in all grades drop off rapidly as T is increased above room T. The time–temperature dependence of the tensile properties in this regime appears dominated by the presence of the α transition at approximately 100°C, which shows similar features to a glass transition.

Financial support from the Swiss Commission pour l'Encouragement de la Recherche Scientifique (CERS) is gratefully acknowledged. Special thanks are also due to H. Terwyen, Hoechst AG, Frankfurt am Main, for his assistance with the injection molding of some of the specimens.

REFERENCES

1. S. G. Cottis, J. Economy, and B. E. Nowak, U.S. Pat. 3,600,350 (1972) (to Carborundum).
2. H. F. Kuhfuss and W. J. Jackson, U.S. Pat. 3,778,410 (1973) (to Eastman-Kodak).
3. G. W. Calundann, (Celanese), U.S. Pat. 4,161,470 (1979).
4. G. W. Calundann and M. Jaffe, in *Proceedings of The Robert A. Welch Foundation Conferences on Chemical*

Research, XXVI, Synthetic Polymers, Houston, Nov., 1982.
5. G. Kirsch and H. Terwyen, *Kunststoffe,* **80,** 1160 (1990).
6. P. Edwards, Mod. Plast. Int., **March,** 32 (1989).
7. S. K. Garg and S. Kenig, in *High Modulus Polymers,* A. Z. Zachariades and R. S. Porter, Eds., Marcel Dekker, New York, 1988.
8. Y. Ide and Z. Ophir, *Poly. Eng. Sci.,* **23,** 261 (1983).
9. G. Menges, T. Schacht, H. Becker, and S. Ott, Int. Polym. Process., **2,** 77 (1987).
10. H. Thapar and M. Bevis, *J. Mat. Sci. Lett.,* **2,** 733 (1983).
11. L. C. Sawyer and M. Jaffe, *J. Mat. Sci.,* **21,** 1897 (1986).
12. E. G. Joseph, G. L. Wilkes, and D. G. Baird, *Polymer,* **26,** 689 (1985).
13. E. G. Joseph, G. L. Wilkes, and D. G. Baird, *Polym. Eng. Sci.,* **25,** 377 (1985).
14. G. G. Viola, D. G. Baird, and G. L. Wilkes, *Polym. Eng. Sci.,* **25,** 888 (1985).
15. T. Weng, A. Hiltner, and E. Baer, *J. Mat. Sci.,* **21,** 744 (1986).
16. S. Kenig, B. Trattner, and H. Andermann, *Polym. Compos.,* **9,** 20 (1988).
17. A. Pirnia and C. S. P. Sung, *Macromolecules,* **21,** 2699 (1988).
18. E. Suokas, J. Sarlin, and P. Törmälä, *Mol. Cryst. Liq. Cryst.,* **153,** 515 (1987).
19. A. Boldizar, *Plast. Rubber Process. Appl.,* **10,** 73 (1988).
20. E. Suokas, *Polymer,* **30,** 1105 (1989).
21. D. J. Blundell, R. A. Chivers, A. D. Curson, J. C. Love, and W. A. MacDonald, *Polymer,* **29,** 1459 (1988).
22. B. Zülle, A. Demarmels, C. J. G. Plummer, T. Schneider, and H.-H. Kausch, *J. Mat. Sci. Lett.,* to appear.
23. B. Zülle, A. Demarmels, C. J. G. Plummer, and H.-H. Kausch, to appear.
24. C. J. G. Plummer, in *Advanced Thermoplastics and their Composites,* H.-H. Kausch, Ed., Hanser, Munich, Chap. 9, to appear.
25. H. Voss and K. Friedrich, *J. Mat. Sci.,* **21,** 2889 (1986).
26. M. Cao and B. Wunderlich, *J. Polym. Sci. Polym. Phys. Ed.,* **23,** 521 (1985).
27. S. Kenig, B. Trattner, and H. Andermann, *Polym. Compos.,* **9,** 20 (1988).
28. C. J. G. Plummer, unpublished results, Lausanne (1991).
29. R. A. Chivers and D. R. Moore, *Polymer,* **32,** 2190 (1991).
30. T. Weng, A. Hiltner, and E. Baer, *J. Compos. Mater.,* **24,** 103 (1990).
31. T. L. Smith, *J. Polym. Sci.,* **20,** 447 (1956).
32. J. D. Ferry, *Viscoelastic Properties of Polymers,* Wiley, New York, 1980.
33. B. Brew, J. Sweeney, R. A. Duckett, and I. M. Ward, in *Proceedings of the 8th International Conference on Yield and Fracture of Polymers,* Cambridge, April 1991, paper 18.

Received May 27, 1992
Accepted July 28, 1992